Material: Ferritic Steel: F82H
Property: Irradiation Temperature (˚C) versus Bubble Density (m^-3)
Condition: Irradiated
Data: Experimental

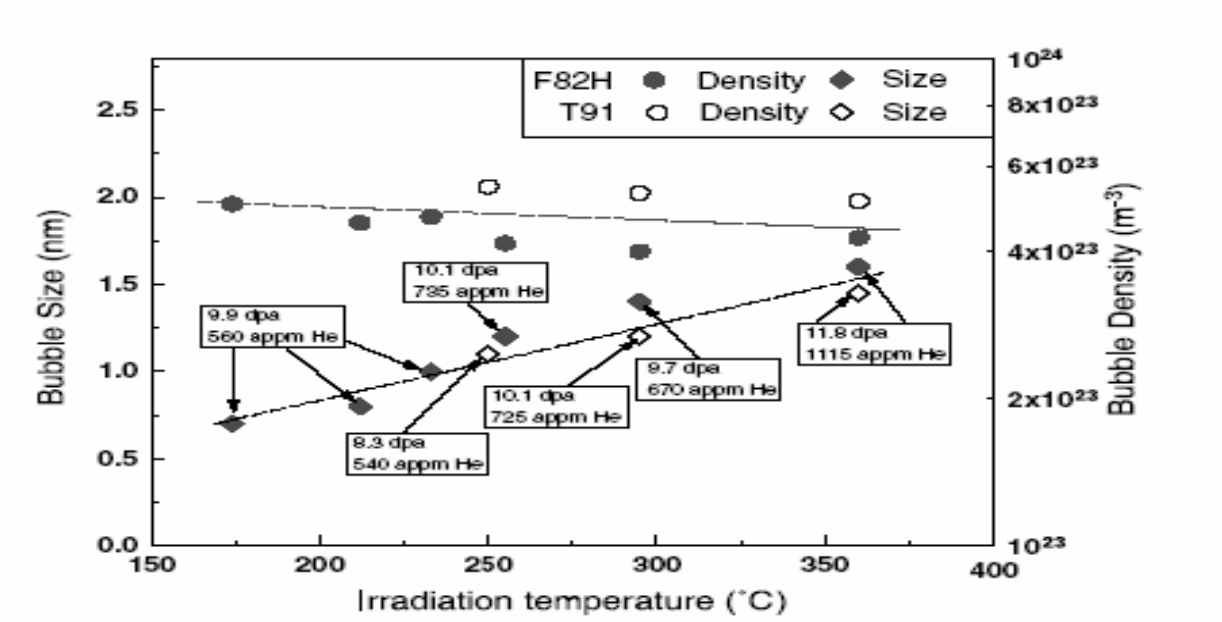

Fig. 8. The temperature dependence of sizes and densities of helium bubbles for T91 and F82H. The irradiation doses and He concentrations are indicated at the size data points.

Source:
Journal of Nuclear Materials, 318, 2003, 207-214

Title of paper (or report) this figure appeared in:
Microstructure in martensitic steels T91 and F82H after irradiation in SINQ Target-3

Author of paper or graph:
X. Jia, Y. Dai

Caption:
The temperature dependence of density of helium bubbles for T91 and F82H.
Note: Figure 2 of 2 indicating the temperature versus density data.

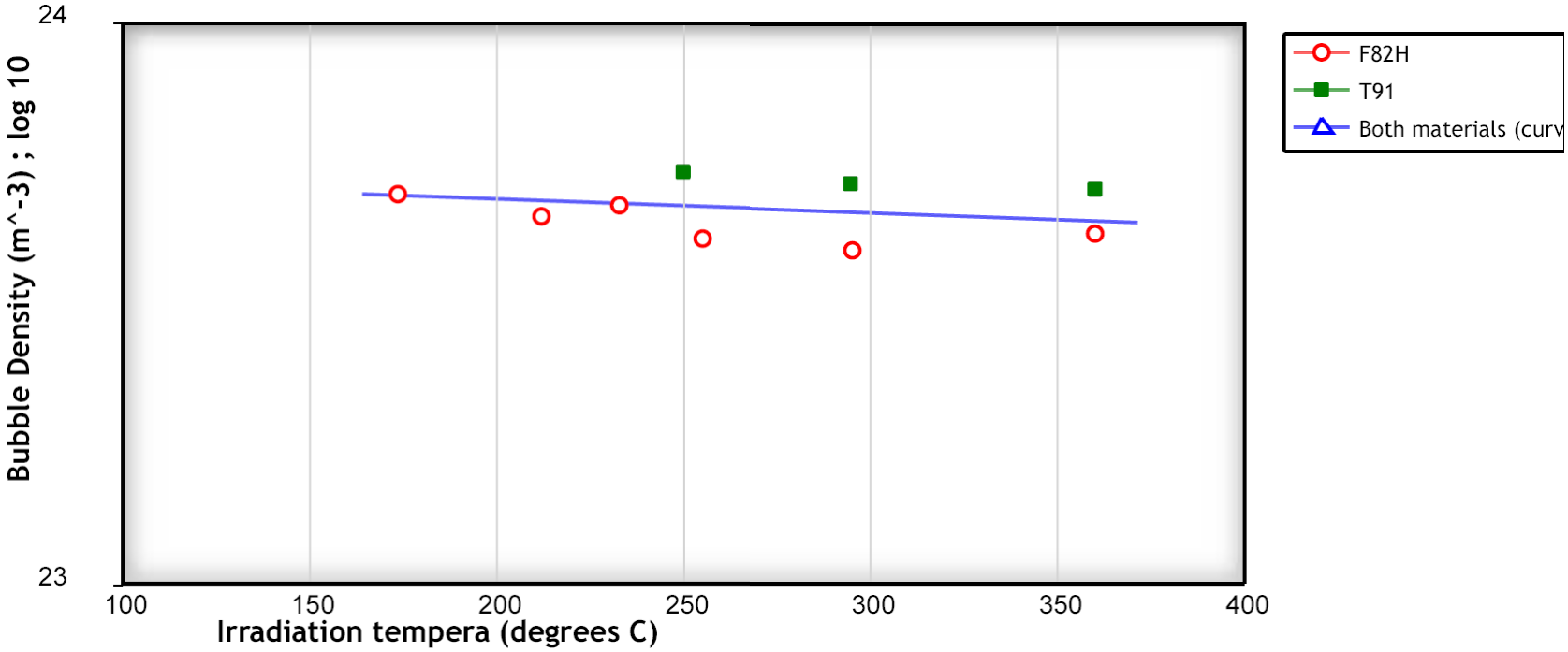

The temperature dependence of density of helium bubbles for T91 and F82H. Note: Figure 2 of 2 indicating the temperature versus density data.

Reference:

Author: *X. Jia, Y. Dai*

Title: *Microstructure in martensitic steels T91 and F82H after irradiation in SINQ Target-3*

Source: *Journal of Nuclear Materials, 2003, Volume 318, Page 207-214*, [PDF]

View Data | Author Comments

Plot Format:

Y-Scale: ○ linear ◉ log ○ ln

X-Scale: ◉ linear ○ log ○ ln

Available online at www.sciencedirect.com
SCIENCE DIRECT®
Journal of Nuclear Materials 329–333 (2004) 309–313
journal of nuclear materials
www.elsevier.com/locate/jnucmat

Microstructure and mechanical properties of F82H weld metal irradiated in SINQ target-3

Xuejun Jia *, Y. Dai

Paul Scherrer Institut, CH-5232 Villigen, PSI, Switzerland

Abstract

The present work is concerned with the microstructure and mechanical behavior of F82H weld metal before and after irradiation to about 11 dpa with simultaneous helium concentrations up to 1000 appm. Optical and TEM observations and micro-hardness test were performed to identify the irradiation effect. Before irradiation, the microstructure of the weld metals is tempered martensite. Precipitates are predominately $M_{23}C_6$ carbides located along martensitic lath boundaries and primary austenite grain boundaries, but some $M_{23}C_6$ carbides rich areas are found. The weld metal has higher dislocation density and also higher hardness than the base metal. Radiation produced a significant change in the microstructure of the weld metal, similar to the F82H base metal irradiated under the same condition. The mean size and the density of defect clusters are comparable to previous results, and the density of helium bubbles is a little higher in the weld metal. The micro-hardness test after irradiation shows significant hardening that does not saturate at higher dose.

1. Introduction

The low-activation ferritic–martensitic steels are candidate materials for the first wall and blanket of fusion reactors due to their lower shift of the ductile-to-brittle transition temperature after neutron irradiation as compared to conventional ferritic–martensitic steels [1,2].

Welding is an inevitable procedure for the fabrication of components. During welding, the cooling rate of the weld metal and the heat-affected zone (HAZ) is very high. Therefore, segregation of alloying elements is prominent and non-equilibrium phases may be present in the weld metal. These factors affect phase transformation in the weld metal during heat treatment. The microstructure and properties of the weld metal are, therefore, different from that of forged and heat-treated base metal.

F82H is among the alloys of the IEA round robin test on reduced-activation ferritic/martensitic (RAFM) steels for fusion structural applications. A lot of work has been done in recent years on the microstructure and mechanical properties of F82H weld metal, but most were concerned mainly with the mechanical properties before and after neutron irradiation [3–8]. This study will evaluate the microstructure and properties of F82H weld metal after an irradiation in the Swiss Spallation Neutron Source (SINQ) target-3 under a proton and neutron mixed spectrum.

2. Experimental

F82H steel (IEA Heat 9741) used in this study was provided by Japan, through the Fusion Technology Materials group (PIREX) of CRPP-EPFL, Switzerland. Its composition is: 7.65 Cr, 2 W, 0.16 Mn, 0.16 V, 0.02 Ta, 0.11 Si and 0.09 C in wt%, and Fe for the balance. The plate was normalized at 1040 °C for 38 min and tempered at 750 ° C for 1 h, which produces a fully martensite structure [9]. The 3.3 mm thick plate was

* Corresponding author. Tel.: +41-56 310 4491; fax: +41-56 310 4529.
E-mail address: xuejun.jia@psi.ch (X. Jia).

0022-3115/$ - see front matter © 2004 Elsevier B.V. All rights reserved.
doi:10.1016/j.jnucmat.2004.04.048

Table 1
Irradiation condition and defect TEM measurement results for F82H weld

Specimen	Dose (dpa)	Helium (appm)	H (appm) (calculated)	Irradiation temperature (°C)	Defect		Bubble	
					Size (nm)	Density (m^{-3})	Size (nm)	Density (m^{-3})
S^{15}	2.2	125	642	68 ± 5	3.8	3.14×10^{22}	–	–
S^{16}	3.8	214	1490	110 ± 10	3.3	3.05×10^{22}	–	–
S^{8}	5.7	375	1880	200 ± 18	3.9	3.10×10^{22}	–	–
S^{10}	10.4	780	3895	245 ± 20	5.8	4.12×10^{22}	1.0	5.03×10^{23}
S^{2}	11.1	1000	4680	345 ± 30	7.5	1.60×10^{22}	1.3	5.31×10^{23}

EB-welded without filler metal. A welding speed of 10 mm/s was achieved with an electron beam of 150 kV and 9 mA. The preheating temperature was 285–300 °C. The post weld heat treatment was performed at 720 °C for 1 h.

TEM disc samples containing the weld area were used in the present study to perform both the microstructure observation and micro-hardness test. The discs were irradiated in SINQ target-3 to 2–12 dpa. The irradiation was performed with a total proton current of about 0.85 mA for first 12 months and about 1.04 mA for the last 2 months of beam time. The difference of the irradiation temperature in these two periods is as great as 15% of the temperature values. The temperature values used in this report are the average values of those in the two periods. More detailed information can be found in Ref. [10]. Table 1 summarizes the information of irradiation doses and temperatures of the samples.

Samples for optical examination were prepared by polishing and etching in Villela reagent. Micro-hardness test was performed by means of Vickers micro-hardness measurements (0.05 Hv) on the TEM discs. Transmission electron microscope (TEM) samples preparation was optimized by using 1 mm techniques, in which the 1 mm disk is punched from the center of the welded zone after etching. TEM investigation of the microstructure was performed at 200 kV on a JEOL 2010 equipped with EDX measurement device. The most often used image conditions were bright field (BF) and weak beam dark-field (WBDF) at **g** (**4g**–**6g**), $\mathbf{g} = 200$ near $= 011$. But only micrographs of **g** (**5g**) were used for quantifying the size and density of defect clusters [11].

3. Results and discussion

3.1. Metallurgical characterizations

Fig. 1(a) shows the cross-sections of the EB welded F82H plate taken from a mini-tensile sample. The width of the weld zone and HAZ is 1 and 0.5 mm respectively. The mean grain size for the base metal is about 30 μm. In the welded zone, the coarse grains are more irregular

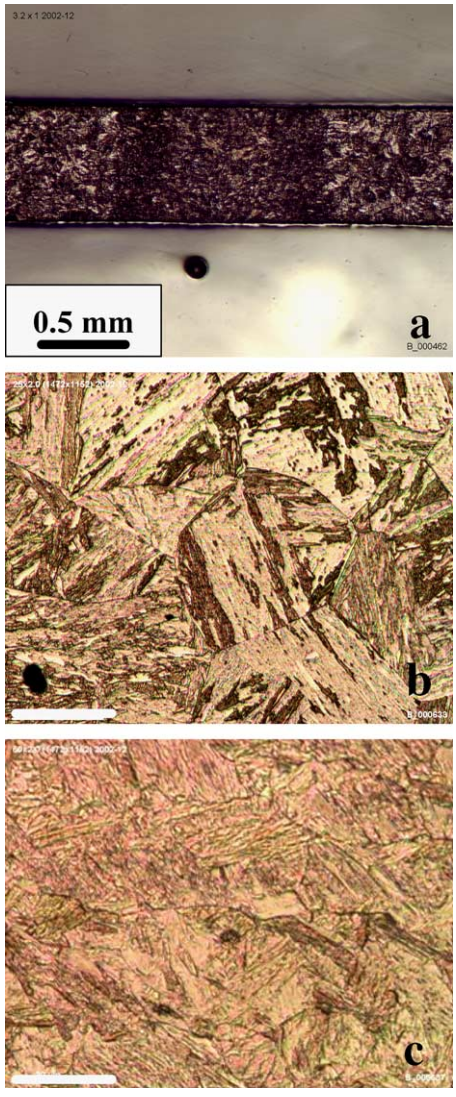

Fig. 1. (a) The cross-section of the EB welded F82H plate (a) and the optical martensitic microstructure of the base metal (b) and the weld metal (c). The scale in (b) and (c) is 20 μm.

and the mean grain size is above 50 μm. Fig. 1(b) and (c) shows the grain structures of the base and WZ metals; both of them are fully martensitic structure with several martensite laths bundles with different orientations in any one grain.

3.2. Micro-hardness test

The micro-hardness data are measured perpendicular to the weld center along the line from base metal, HAZ and weld zone. The hardness value of F82H base metal is around 220–230 Hv measured with a test weight of 0.05 N. Hardening in the weld metal and the adjacent HAZ is more clearly observed and gives a value about 290–320 Hv. Welding heat affects the weld joint both in hardening and softening. F82H is quench hardenable so that the cooling of the weld metal and surrounding HAZ from the austenitic region easily makes a fully martensitic structure, which is harder than the base metal.

After irradiation, significant irradiation hardening was found by the micro-hardness test. The hardening increases with increasing dose and does not saturate at doses up to 11 dpa, as shown in Fig. 2. This result has the same trend for the irradiation hardening as the tensile test results obtained from several ferritic/martensitic steels irradiated with high-energy protons [2,12,13].

3.3. Microstructure

Fig. 3(a)–(d) shows the microstructure of the F82H base metal and the weld metal before irradiation. The microstructure of the base metal prior to irradiation has a typical tempered martensitic lath structure containing dislocations with a density of approximately 1×10^{14} m^{-2}. $M_{23}C_6$ type precipitates located mainly along prior austenite grain boundaries and martensite lath boundaries. The size of precipitates varied from about 0.01–0.5 μm, as show in Fig. 3(a) and (c) respectively. Fig. 3(b) and (d) shows the same pictures for weld metal, showing the weld metal also has the typical tempered martensitic lath structure after the post-welding tempering. The difference is that the weld metal has larger mean prior austenite grain size (above 50 μm) compared to base metal which is about 30 μm, and the dislocation density in the weld metal is about 2.23×10^{14} m^{-2}, much higher than that in the base metal.

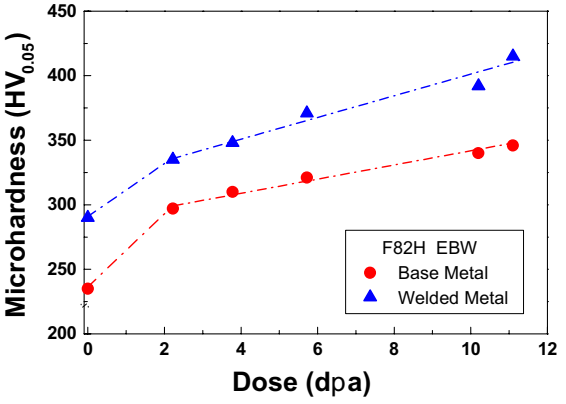

Fig. 2. Micro-hardness of the base and the weld metal before and after irradiation.

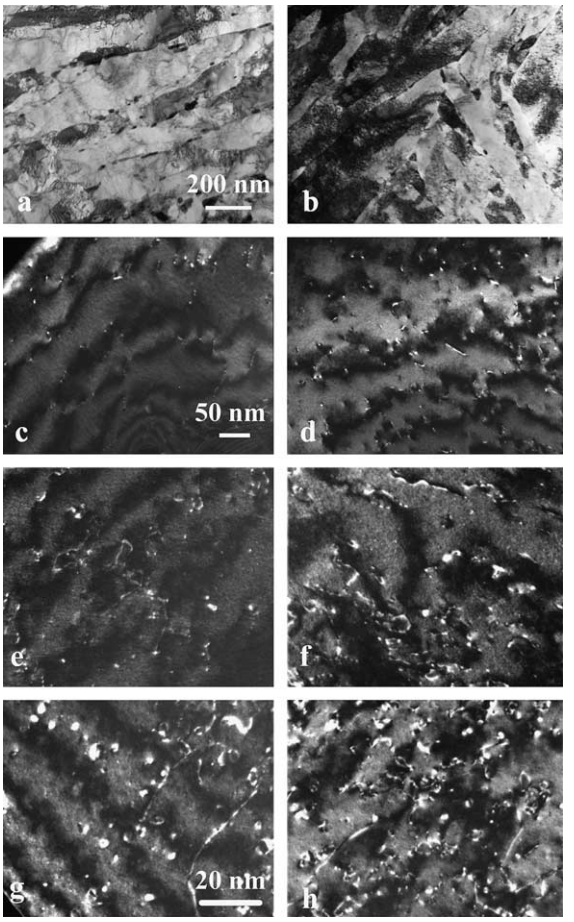

Fig. 3. The microstructure of the F82H base metal and weld metal before and after irradiation: (a) base metal, BF; (b) weld metal, BF; (c) base metal, WBDF and (d) weld metal, WBDF; (e) and (g) base metal, 4.7 dpa/110 °C and 10.1 dpa/55 °C; (f) and (h) weld metal, 3.8 dpa/110 °C and 10.4 dpa/245 °C, respectively. The scale in (a) is 200 nm for (a) and (b), the scale in (c) is 50 nm for (c) and (d) and the scale in (e) is 20 nm for others.

Fig. 3(e)–(h) shows the irradiated microstructures of F82H–EBW, together with our previous results for the F82H base metal irradiated in the same irradiation conditions [14]. The comparison shows that there is not

much difference between the radiation-induced defect cluster structures. Namely, at low irradiation dose and temperature, microstructure is dominated by very small defect clusters (black dots or small interstitial loops), as shown in Fig. 3(e) and (f). With increasing irradiation dose, the defect cluster size and density increase, as show in Fig. 3(g)–(h). But at the highest irradiation does, because of the higher irradiation temperature, the defect density decreases and the mean size increase significantly.

Fig. 4 gives the dose dependence of the size and density of defect clusters in the F82H weld metal. The data for F82H base metal from previous results was also plotted as a comparison. The density and the mean size of defect clusters in the weld metal are comparable with the base metal.

As observed in the base metal, helium bubble structure was also found in the weld metal at higher irradiation doses with higher irradiation temperature. Compared to the base metal, the bubble density was higher in the weld metal as result of the higher dislocation density. These dislocations act as sinks for the interstitial clusters and allow the vacancies to aggregate to form small voids; these small voids finally become the sinks for the transmutation helium produced under spallation conditions. The helium bubble structure is visible under TEM at higher helium concentrations and higher irradiation temperatures. Meanwhile, the mean bubble size is similar to that of the base metal.

The most important difference in microstructure between the weld metal and the base metal is the structure of the precipitates. Fig. 5 shows a precipitate-rich area in an irradiated samples. The area is a few μm large, and EDS analysis shows that precipitates are rich in Cr (~50–59%) and Fe (~33–39%), with lower Mn, Ni, V, W and Si contents. Diffraction patterns of the precipitates show an fcc crystal structure with a lattice parameter $a = 1.06$ nm, indicating that they are $M_{23}C_6$ type carbides. The percentage of Fe is higher in the center of the area and decrease from the center to the edge, and the percentage of Cr is higher at the edge and decrease from the edge to the center. The relatively Fe-rich nature of the $M_{23}C_6$ carbides in the center of the precipitates-rich area could be attributed to the relatively fast cooling rate and insufficient time for chromium to diffuse into the center of the precipitates-rich area.

The reason why such precipitate-rich areas appear is not so clear yet and we did not find any of them in the base metal. Due to the lower irradiation temperature in those samples, radiation-induced segregation (RIS) and radiation-induced precipitation should not occur [2]. The most probable reason could be due to the heterogeneous distribution of alloying elements during the welding procedure. As we know, compared with the base metals, the distribution of alloying elements in a weld metal is more heterogeneous. Consequently, the microstructure of the weld metal, including precipitates and matrix, is obviously inhomogeneous. Nevertheless, coarse $M_{23}C_6$ carbides are very detrimental to the toughness of the weld metal and must be avoided.

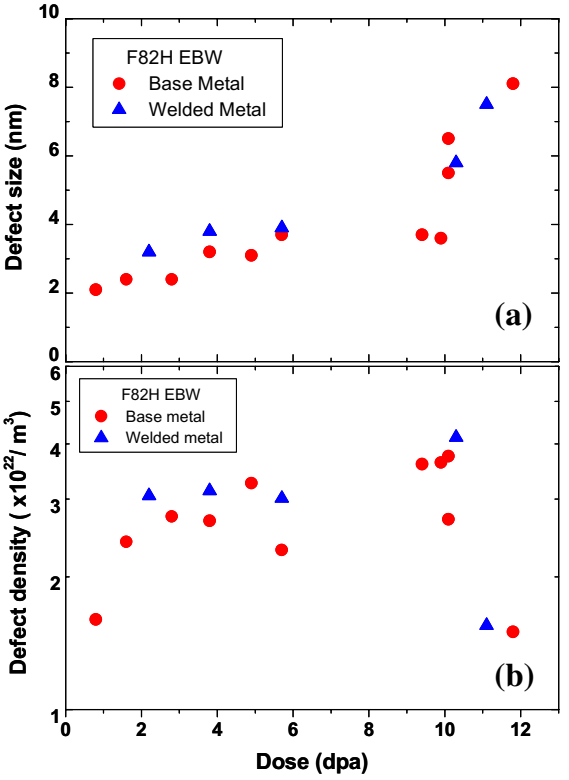

Fig. 4. Dose dependence of the size (a) and density (b) of defect clusters in F82H weld metal.

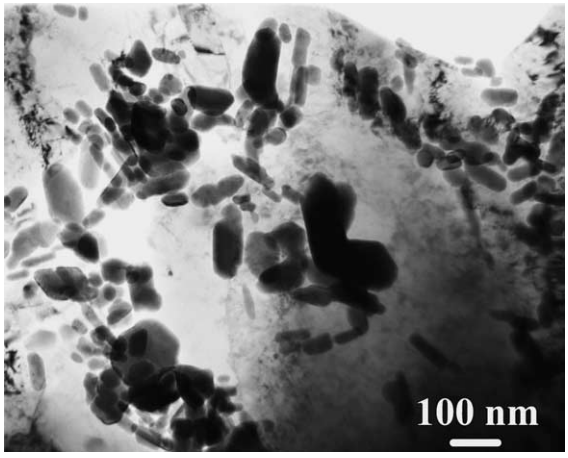

Fig. 5. The precipitate-rich area in an irradiated F82H weld metal sample.

4. Conclusion

1. The microstructure of the weld metal has a typical tempered martensitic laths structure. Precipitates in the weld metals are predominately $M_{23}C_6$ carbides, and mainly distributed along the martensitic lath boundaries and primary austenite grain boundaries, but some $M_{23}C_6$ carbides rich areas exist.
2. The dislocation density in the weld metal is higher than in the base metal. Meanwhile, micro-hardness test shows a higher hardness value of the weld metal.
3. The irradiation produced a significant change in the microstructure of the weld metal, as observed in the F82H base metal irradiated under the same conditions in the previous work. Small defects namely as black dots and faulted Frank interstitial loops are found in the irradiated samples, the density and the mean size of the defects are comparable with the previous results.
4. A high density of helium bubbles is observed in the case of higher irradiation doses and higher temperatures. The density of bubbles is slightly higher than that in the weld metal.
5. The micro-hardness test after irradiation shows significant hardening, and the hardening does not saturate at irradiation doses up to 11 dpa.

Acknowledgements

This work is included in both SPIRE (irradiation effects in martensitic steels under neutron and proton mixed spectrum), subprogram of the European Fifth Framework Program, which are supported by Swiss Bundesamt feur Bildung und Wissenchaft.

References

[1] S.N. Rosenwasser, P. Miller, J.A. Dalessandro, J.M. Rawls, W.E. Toffolo, W. Chen, J. Nucl. Mater. 85&86 (1979) 177.
[2] R. Klueh, D.R. Harries, High-chromium ferritic and martensitic steels for nuclear application, ASTM stock number: MONO3; ISBN 0-8031-2090-7.
[3] R. Mythili, V. Thomas Paul, S. Saroja, M. Vijayalakshmi, V.S. Raghunathan, J. Nucl. Mater. 312 (2003) 199.
[4] A. Alamo, A. Castaing, A. Fontes, P. Wident, J. Nucl. Mater. 283–287 (2000) 1192.
[5] T. Sawai, K. Shiba, A. Hishinuma, J. Nucl. Mater. 283–287 (2000) 657.
[6] G.J. Cai, Microstructure and mechanical properties of high chromium steel weld metals, Thesis No.1012, Goeteborg 1994, Sweden.
[7] J. Rensman, E.V. van Osch, M.G. Horsten, D.G. d'Hulst, J. Nucl. Mater. 283–287 (2000) 1201.
[8] S. Kaga, T. Tamura, H. Yoshida, K. Miyata, J. Nucl. Mater. 179–181 (1991) 588.
[9] Y. Kohno, D.S. Gelles, A. Kohyama, M. Tamura, A. Hishinuma, J. Nucl. Mater. 191–194 (1992) 868.
[10] Y. Dai, G. Bauer, J. Nucl. Mater. 296 (2001) 43.
[11] X. Jia, Y. Dai, M. Victoria, J. Nucl. Mater. 305 (2002) 1.
[12] Y. Dai, X. Jia, K. Farrell, J. Nucl. Mater. 318 (2003) 192.
[13] K. Farrell, T.S. Byun, J. Nucl. Mater. 318 (2003) 274.
[14] X. Jia, Y. Dai, J. Nucl. Mater. 318 (2003) 207.